Flash nanoprecipitation of hafnia nanoparticle computed tomography contrast agent

Sitong Liu[1], Matthew Po[1], Anahita Heshmat[2], Evan Anguish[3], Jennifer Andrew[3], and Carlos M Rinaldi-Ramos[1,4,+]

Affiliations:

1. Department of Chemical Engineering, University of Florida, Gainesville, FL 32611, United States of America
2. Department of Radiology, University of Florida, Gainesville, FL 32610-0374, United States of America
3. Department of Material Science and Engineering, University of Florida, Gainesville, FL 32603, United States of America
4. J. Crayton Pruitt Family Department of Biomedical Engineering, University of Florida, Gainesville, FL 32611-6131, United States of America

[+]Corresponding author

Corresponding author email address: Carlos.Rinaldi@ufl.edu

Abstract:

Hafnium oxide (hafnia) nanoparticles have recently attracted attention for their application as computed tomography (CT) contrast agents due to their high X-ray attenuation and low cost. Here we employ flash nanoprecipitation (FNP) to formulate hafnia nanoclusters (HNCs) consisting of a core of precipitated individual hafnia nanoparticles and polylactic acid homopolymer and an outer coating of the block copolymer polylactic acid-b-polyethylene glycol (PLA-b-PEG). The HNCs can be produced with controlled hydrodynamic size in the range of 100-300 nm using a simple 3D-printed FNP mixer. The CT performance of the HNCs was evaluated in a pre-clinical small animal scanner and in a clinical scanner. In both systems the HNCs displayed ~1.5x greater contrast compared to the commercial iodinated molecular contrast agent Omnipaque used clinically.

Keywords: hafnium oxide; nanoparticle; flash nanoprecipitation; computed tomography; contrast agents.

Acknowledgements

This was supported by the US National Science Foundation through grant DMR-1832733.

Statements and Declarations

Competing interests: The authors have declared that no competing interest exists.

1. Introduction

Computed tomography is a clinically available and widely used medical imaging technique. Because of its safety and cost-effectiveness, CT has been used clinically for decades to help in both diagnosis and therapy. According to Harvard Medical School[1], over 80 million CT scans are performed in the United States each year, accounting for 50 – 75% of all medical imaging done. CT relies on the 3D reconstruction of X-ray images taken by rotating the detector and X-ray source around an object to be imaged[2]. Due to the absorption or scattering of photoelectrons, X-rays undergo attenuation while traveling through an object, resulting in a loss of beam intensity. The contrast in X-ray imaging is derived from differences in mass attenuation between tissues. Structures like bone are dense and generate a greater signal, making them easy to see in X-ray images, while soft materials like tissue are much less dense and harder to observe. Thus, contrast agents are often necessary to illuminate areas of interest, especially in soft tissues or regions where soft tissue is intermingled with denser material.

The most used, clinically available radiopaque element in X-ray imaging is iodine (Z=53) because of its high atomic number compared to biological tissues[3, 4]. However, according to simulations[5] and experimentation[6], iodinated molecules are not optimal for CT compared to high atomic number (Z) metals, such as gold (Z=79) and hafnium (Z=72). As a result, studies on hafnium and gold-containing materials as CT contrast agents have gained recent interest. For example, the hafnium-containing contrast agent BAY-576 has been reported to have better CT contrast than the iodinated contrast agent iopromide[7]. However, BAY-576 is excreted quickly via the kidneys and requires a high dose to maintain constant visualization in CT[8]. Other types of contrast agents incorporating high Z metals include metal and metal oxide nanoparticles, such as gold[9, 10], hafnium oxide[6, 11, 12], and hafnium-containing metal-organic frameworks[13]. AuroVist™ 15 nm, a gold nanoparticle agent, has been shown to provide better contrast than Iomeron, an iodinated contrast agent, in blood and can be used for blood pool imaging purposes[14, 15]. Although other gold nanoparticles have also been reported for use as CT contrast agents, hafnium based contrast agents provide a much more affordable choice[16, 17]. Hafnia nanoparticles of physical size from 7 to 30 nm were first introduced as CT contrast agents in 2016[6], though the reported nanoparticles appear to be agglomerated with hydrodynamic diameter of >200 nm and poor stability[18]. Other studies have reported hafnia CT contrast agents with hydrodynamic sizes below 100 nm[12, 19]. Control over nanoparticle CT contrast agents in the hydrodynamic size range of 100 to 300 nm with good CT contrast is desirable because nanoparticle size is one of the most important factors affecting their pharmacokinetics and cellular interaction[20].

Size tunability of the nanoparticles can be attained through modifying synthesis parameters[21, 22]. However, the achievable size range with synthesis parameter adjustment is narrow (from nanometers to tens of nanometers). Furthermore, the chemical synthesis of hafnia nanoparticles is relatively new and current methods do not afford fine control over hafnia nanoparticle size. A simple and scalable alternative route for fabricating composite nanoparticles containing hafnia nanoparticles over a wide size range (100s of nm) is therefore desirable.

Flash nanoprecipitation (FNP) is a scalable method to formulate nanoparticles consisting of a hydrophobic core and an outer hydrophilic layer through rapid mixing and diffusion-limited aggregation of hydrophobic materials and amphiphilic block copolymers. Owing to its simplicity, scalability, manufacturability, high loading and encapsulation efficiency, and potential to encapsulate multiple hydrophobic materials, FNP has been used to produce nanoclusters for biomedical applications[23-25]. Studies leveraging FNP to encapsulate inorganic nanoparticles, such as iron oxide and gold, have been used to formulate composite nanoparticles for drug delivery[23] and for use in magnetic particle imaging[26] and magnetic resonance imaging[24]. Here, we apply FNP for the scalable formulation of hafnia CT contrast agents with tunable size.

We report the formulation of hafnia composite nanoparticles (HNCs) through FNP with homopolymer and block copolymer, achieving a wide range of hydrodynamic diameters. A custom-designed 3D printed multi-inlet-vortex-mixer, pusher, and plunger were used for the FNP process. The physical appearance, hydrodynamic properties, and computed tomography performance of the HNCs were evaluated. The HNCs were also compared to a clinically available iodine-based contrast agent (Omnipaque) in a small animal CT imaging system and in a clinical CT imaging system.

2. Methods

Materials:
Hafnium (IV) tetrachloride (99.9%), trifluoroacetic acid (reagent grade), toluene (>99.5%, ACS reagent), ethanol (200 proof), isopropanol (99%), tetrahydrofuran (THF, 99.8%, HPLC grade, unstabilized), Spectrum™ Spectra/Por Biotech-Grade RC Dialysis Membrane Tubing (100 kDa), MilliporeSigma™ Amicon™ Ultra Centrifugal Filter Units (100 kDa), and acetone (certified ACS) were purchased from Thermo Fisher Scientific (Waltham, MA). Oleylamine (70%, technical grade) was purchased from Sigma-Aldrich (St. Louis, MO). Formlabs Clear V4 resin was purchased from Formlabs (Somerville, MA). Polylactic acid-b-Polyethylene glycol (PLA-b-PEG, 6 kDa PLA, 4.9 kDa PEG) was purchased from Evonik Industries (Essen, Germany). Poly (D,L-lactide) (PLA,

10.3 kDa) was purchased from Polymer Source (Quebec, Canada). Copper TEM grid (carbon film only, 200 mesh) was purchased from TED PELLA, INC (Redding, CA). Omnipaque Contrast Solution (240 mg/mL) was purchased from Patterson Veterinary Supply (Devens, MA). Plastic pot jars round clear leak-proof (6 pack, 1oz) was purchased from Amazon (Seattle, WA)

2.1. Particle synthesis

Synthesis of trifluoroacetate hafnium:
Trifluoroacetate hafnium (IV) was synthesized following the protocol previously described by Liu et al. with minor modifications[27]. Hafnium (IV) chloride (9.6 g) was charged to a 100 mL 3-neck reactor. The flask was equipped with an overhead stirrer in the middle neck, a septum with a thermocouple, and a stainless steel (SS) needle through the left neck. Argon (50 sccm) was supplied continuously through the SS needle during synthesis, using a mass flow controller. Trifluoroacetic acid (50 mL) was added to the reactor slowly, for 1 min, while stirring at 100 rpm. The stirrer rate was changed to 300 rpm after the addition of trifluoroacetic acid. A condenser connected to a chiller was attached to the right neck and the top of the condenser was connected to a standard backflow prevention setup with a water-filled beaker. The reaction mixture was heated to a temperature of 40 °C at a rate of 5 °C/min using a heating mantle followed by soaking for 5 hours. At the end of the reaction, the reaction mixture was transferred to a 100 mL 1-neck round bottom flask for rotary evaporation to remove excess trifluoroacetic acid for 3 hours. The resulting white solid trifluoroacetate hafnium (IV) was stored in a vacuum desiccator until used for nanoparticle synthesis.

Synthesis of hafnia nanoparticles:
Hafnia nanoparticles were synthesized as previously described with some modifications[27]. Trifluoroacetate hafnium (IV) (2.54 g) and oleylamine (53 mL) were added to a 100 mL three-neck reactor. The flask was equipped with an overhead stirrer in the middle neck and a septum with a SS needle through the left neck. A molten metal bath and temperature controller were used as the heating source. The molten metal was heated to 110 °C before pushing the reaction vessel into the molten metal bath. The reaction mixture was soaked for 30 min at 110 °C before heating to 330 °C in 60 min. Argon (100 sccm) was supplied continuously through the SS needle, controlled using a mass flow controller. Uniform mixing at 350 rpm was maintained throughout the reaction. The reaction was stopped after 1 hour since reaching temperature and the reactor was removed from the molten metal bath. Acetone (1x) was used to precipitate the particles at a ratio of 3:1 before toluene and ethanol (3x) in a 1:2 volume ratio was used. Purified oleylamine coated particles were suspended in toluene and stored at 4 °C before use. Thermogravimetric analysis (TGA) was used to determine the hafnium concentration in toluene. 100 µl of particle suspension was added to a pre-weighed empty glass vial before drying overnight and measuring the mass of the dried particles. TGA was then performed on 5-10 mg of dried particle for inorganic percentage. The mass loss below 200 °C was considered moisture and solvent and not included when performing calculations. The organic mass percentage was determined by the weight loss percentage between 200 °C and 550 °C. This inorganic percentage was then applied to the total dry mass to obtain particle mass in 100 µl of particle solution. The concentration of hafnium in the solution was then calculated. Toluene suspension containing 4.5 mg of hafnia nanoparticles (based on TGA as mentioned) was measured into 4 mL dry, empty glass vials before placed in a vacuum oven overnight to remove toluene and then placed in a vacuum desiccator for storage before being used in flash nanoprecipitation (FNP).

2.2. Composite particle fabrication

Multi-inlet-vortex-mixer design:
To perform flash nanoprecipitation, a multi-inlet-vortex-mixer (MIVM) was designed using the online, three-dimensional (3D) computer-aided design program Onshape (Onshape, MA, USA) and 3D printed with the Form 3 stereolithography printer (Formlabs, MA, USA). The dimensions used in designing the 3D printed MIVM were based on a prior study[28]. The designed 3D printable MIVM is shown in Figure S1. The MIVMs were printed on a Form 3 printer (Formlabs, MA, USA) using Clear V4 resin (Formlabs, MA, USA) with layer sizes of 50 µm. A custom-built holder and sleeve, shown in Figure S2, were also designed, and printed.

Flash nanoprecipitation for assembly of hafnia nanoparticle clusters (HNCs):
A typical procedure for producing HNCs by FNP was performed as follows. For small-scale HNCs fabrication, 25 mg of PLA-b-PEG was weighed in a dry, empty 4 ml glass vial before the addition of THF for preparation of 10 mg/mL suspension. In a separate dry empty 4 ml glass vial, 1.5 mg/mL hafnia nanoparticles suspended in THF was prepared. Loading of 2 mL of hafnia nanoparticle THF suspension, 2 mL PLA-b-PEG THF suspension, and two 2 mL DI water into four 5 mL syringes were then performed. Four syringes were connected to the MIVM with two water syringes opposite to each other and were pushed through the MIVM at approximately 60 mL /min. This flow rate was chosen based on a prior study that suggests that reproducible and narrow size distribution composite nanoparticles are fabricated at a such high flow rate [28]. The resulting product was recovered in a 100 mL vial with 36 mL of deionized water present in the vial before catching the FNP product. For removal of THF, dialysis against water for 24 hours was performed using Spectrum™ Spectra/Por Biotech-Grade RC Dialysis Membrane Tubing (100 kDa). For large-scale HNCs fabrication, 30 ml of each stream was used during the FNP with 50 ml gaslight syringes (Hamilton) and syringe pumps (Harvard Apparatus). For

FNPs with PLA as the co-core polymer, various mass concentrations were prepared by the addition of PLA in the hafnia nanoparticle THF suspension. For the concentration of HNCs after dialysis, MilliporeSigma™ Amicon™ Ultra Centrifugal Filter Units (100 kDa) were used with centrifugation. Final hafnia concentration in HNCs water suspension was quantified by TGA as previously explained.

2.3. Physical and Hydrodynamic Properties Characterization

2.3.1. Transmission Electron Microscopy

Images of hafnia particles sampled on 200-mesh copper grids with carbon film were acquired using a FEI Talos™ F200i S/TEM. Physical diameters (D_p) were obtained by analyzing the images using Fiji.[29] Reported size distribution statistics and histograms are based on at least 200 particles.
The number median diameter (D_{pg}) and geometric standard deviation ($\ln \sigma_g$) of the particle size distribution were obtained by fitting the size distribution histograms to the lognormal distribution ($n_N(D_p)$) using[30]

$$n_N(D_p) = \frac{1}{\sqrt{2\pi} D_p \ln \sigma_g} \exp\left(-\frac{\ln^2 D_p/D_{pg}}{2 \ln^2 \sigma_g}\right) \quad (1)$$

The composition of the hafnia nanoparticles was analyzed using energy-dispersive X-ray spectroscopy (EDS). The FEI Talos™ F200i S/TEM was equipped with a Bruker XFlash™ 6T/30 windowless silicon drift detector EDS system. The EDS spectrum was obtained in TEM mode.

2.3.2. Crystallographic Characterization

XRD analysis was performed on purified and dried hafnia nanoparticles to determine their crystal structure. To obtain XRD spectra of the hafnia nanoparticles, dried particles were deposited onto a glass slide. The diffraction spectra were obtained on a Panalytical X'Pert MPD powder diffractometer with an 1800 W Cu anode. The Kα line of Cu (0.154 nm) was chosen as the source of the monochromatic radiation. The sample was scanned over a range of 20 to 100 ° in 2θ coordinates with a step size of 0.008 °, and 40 s was chosen to be the time per step. The data was compared to JCPDS standards for monoclinic phases (00-034-0104) of hafnia.

2.3.3. Dynamic Light Scattering and Zeta Potential

A Brookhaven Instruments 90Plus/BI-MAS dynamic light scattering and zeta potential measurement instrument, operating at a scattering angle of 90° at room temperature, was used to determine the hydrodynamic size and zeta potential of the HNCs. For hydrodynamic diameter measurements, particles at 1 mg/ml were suspended in 1 ml of deionized water, resulting in a final concentration of 0.02 mg/ml. The zeta potential of the particles was measured in a 1 mM KNO3 solution at pH 7, adjusted with nitric acid and potassium hydroxide.

2.4. CT performance

2.4.1. IVIS® Spectrum In Vivo Imaging System

Sample holder design:
To image samples in the IVIS® Spectrum In Vivo Imaging System, sample holders were designed using the online three-dimensional (3D) computer aided design program Onshape (Onshape, MA, USA) and 3D printed with the Form 3 stereolithography printer (Formlabs, MA, USA). The holder was printed using Clear V4 resin (Formlabs, MA, USA) with layer size of 100 µm. CT measurements were performed on samples in 0.2 mL microcentrifuge tubes utilized sample holders which held the tubes vertically. These microcentrifuge tube holders each hold up to 5 tubes. Each microcentrifuge tube rests in a 6.82 mm diameter bore, and the bores have a center-to-center spacing of 11.20 mm. The vertical configuration of this model is shown in Figure S3.

Method of acquisition:
200 µl of each contrast agent (HNCs and Omnipaque) was placed in a 0.2 ml microcentrifuge tube in triplicate, the microcentrifuge tubes were placed in the 3D printed sample holder and the sample was centered in the FOV. Water was also prepared in the same way to provide the control signal. Then, the CT images were scanned in the IVIS® Spectrum In Vivo Imaging System. The specifications for the measurements were: CT only, standard one mouse, voltage 50 kV, current 1 mA, medium resolution.

Method of image analysis:
Images obtained from the CT were stored as DICOM files. Each DICOM file contained data from a set of three vials in the dilution series. These DICOM files were analyzed using 3D Slicer to quantify the CT attenuation of each dilution. First, images were

processed to allow for visualization of the vial contents. Particularly, a threshold was applied to each image followed by a volume rendering of the samples. After visualization was complete, segmentation was performed on each image to identify the contents of each individual vial and mark it for further analysis. Once each segmentation was obtained, segmentation statistics were calculated through the software. For each vial (segmentation), the mean intensity of the signal was reported in the segmentation statistics. These mean intensities were averaged across each dilution to obtain the average intensity for the dilution. Because the IVIS® Spectrum In Vivo Imaging System does not provide CT signal in a way that can be used to calculate X-ray attenuation in HU, no such calculation was conducted. The signal intensity was presented throughout instead to provide quantitative analysis.

2.4.2. Clinical CT

Sample holder design:
To image samples in the Aquilion ONE GENESIS scanner, a sample holder compatible with plastic pot jars was designed using the online three-dimensional (3D) computer-aided design program Onshape (Onshape, MA, USA) and 3D printed with the Form 3 stereolithography printer (Formlabs, MA, USA). The holder was printed using Clear V4 resin (Formlabs, MA, USA) with layer size of 100 µm. CT measurements were performed on samples in 0.2 mL microcentrifuge tubes using sample holders which held the tubes vertically. These microcentrifuge tube holders each hold up to 6 tubes. Each microcentrifuge tube rests in a 41.6 mm diameter bore, and the bores have a center-to-center spacing of 11.0 mm. The configuration of this holder is shown in Figure S4. The fitting of the sample holder in a plastic jar is shown in Figure S5.

Method of acquisition:
To acquire the images, samples (HNCs and Omnipaque) were filled into 200 µl microcentrifuge tubes with a variety of hafnia or iodine concentrations (1 mM to 50 mM). Note that the real volume of liquid that can be added to a 200 µl microcentrifuge tube is close to 300 µl. The sample holder with the microcentrifuge tubes was put into a plastic transparent jar to facilitate image acquisition. The jar was filled with water and closed tightly. The phantom was scanned with a 320-detector CT Scanner (Canon Aquilion ONE Genesis-Edition, Canon Medical Systems USA, Inc., Tustin, CA). The clinical subtraction CT (SCT) head and neck protocol was used to assess the CT numbers of the contrast agents. The specifics of the protocol for SCT are the followings: tube voltage, 120 kVp; $CTDI_{vol}$, 31.4 mGy Body; tube current, 400 mA; rotation time, 0.5 s; field of view, 220.3 mm; Bowtie Filter Size, S; reconstruction kernel, FC64; iterative reconstruction method, AIDR-3D (mild strength); slice thickness, 3 mm; pitch, 0.625; field of view, 200*200 mm^2; detector configuration, 320*0.5 mm. Two scans were acquired for the SCT protocol, as it requires pre- and post-contrast images. The phantom jar with just water was scanned for the initial non-contrast image. The contrast images were acquired with the microcentrifuge tubes containing different contrast agents for the post-contrast scans.

Method of image analysis:
All images were evaluated quantitatively with a MATLAB® (MathWorks, MA, USA) script to extract regions of interest (ROIs) of each contrast agent at various concentrations. The mean CT numbers and standard deviations were collected.

2.5. Colloidal stability

DLS measurements were used to evaluate the colloidal stability of the HNCs in various media. In a plastic DLS cuvette, 1 ml liquid was added from different media with the HNCs at a concentration of 0.025 mg/ml. The media includes phosphate buffered saline (PBS), DMEM, and DMEM + 10% fetal bovine serum (FBS), plus DI wafer as control. The visual appearance of the liquid was observed and the DLS measurements were performed at different time points including 0, 1, 6, 12, and 24 hours.

3. Results and Discussion

3.1. Hafnia nanoparticle synthesis, composite particle fabrication, and characterization

The synthesized hafnia nanoparticles were evaluated using transmission electron microscopy (TEM). As shown in Figure 1a, the hafnia nanoparticles are single cores with a narrow size distribution. The number weighted median physical diameter and the standard deviation were 4.95 nm and 0.15 nm, respectively. The histogram of the physical size and distribution is shown in Figure S6. Energy-dispersive X-ray spectroscopy (EDS) under TEM was performed to verify sample composition and the presence of hafnium in the samples (Figure S7). As seen in Figure S7, the highest peaks come from carbon. This is due to the pure carbon film used for TEM sample preparation. The next highest peaks come from hafnium and oxygen, corresponding to the hafnia nanoparticles. Copper is also present due to the copper grid. Other minor peaks indicate the presence of zirconium, iron, and cobalt. It is common to have small amounts of these metal elements present in hafnium chloride (used for the synthesis of hafnium trifluoroacetate precursor) due to difficulty in their separation during manufacturing.

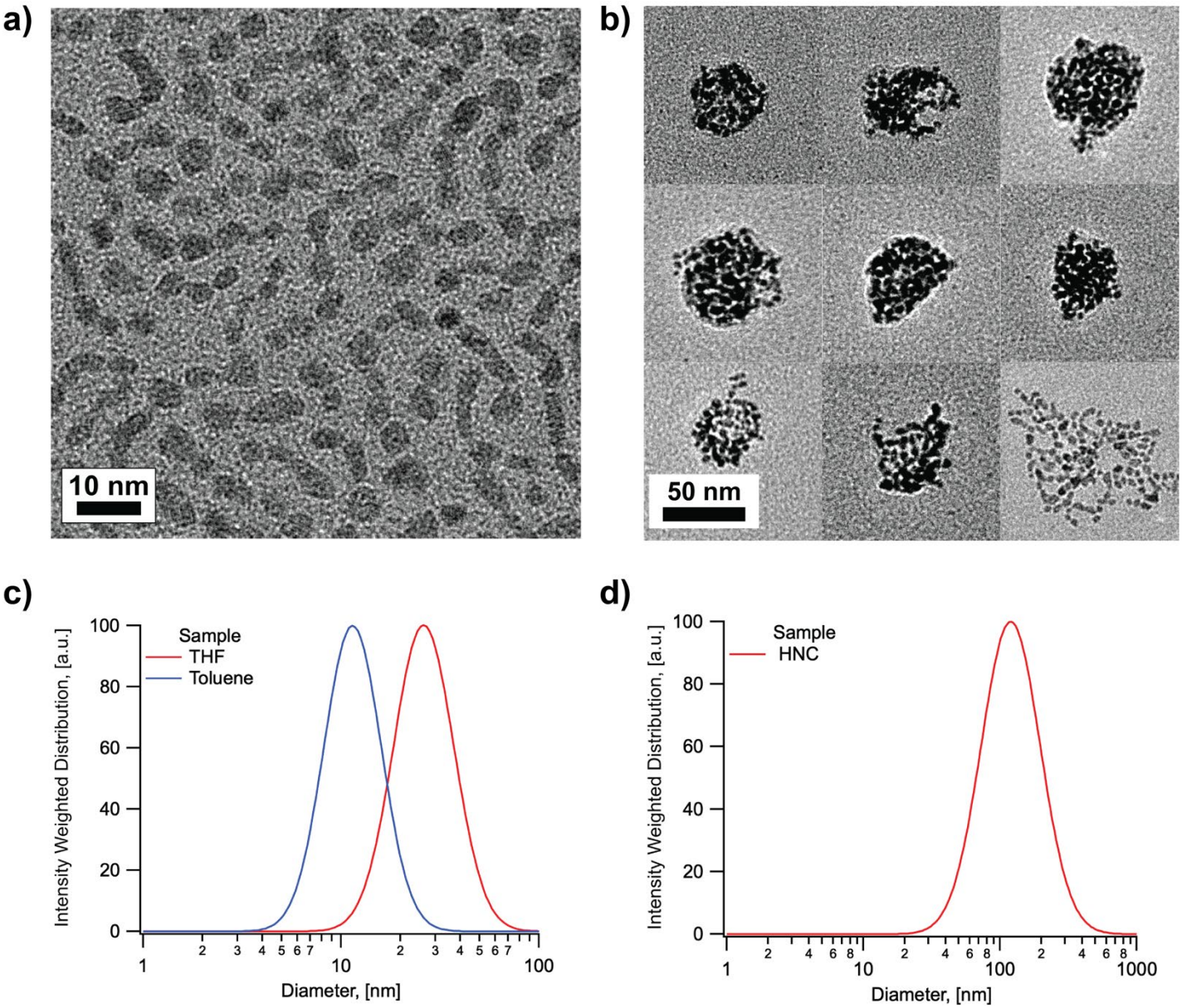

Figure 1. Contrast agent evaluation via transmission electron microscopy (TEM) and dynamic light scattering (DLS). a) Representative TEM images of hafnia nanoparticles. b) A collage image composited of 9 different HNCs imaged via TEM. c) Hydrodynamic diameter distribution of hafnia nanoparticles suspended in toluene and THF. d) Hydrodynamic diameter distribution of HNCs suspended in DI water.

The crystal phase of the nanoparticles was studied using XRD and compared with the JCPDS standard (00-034-0104), suggesting monoclinic phase hafnia (Figure S8). It is worth noting that CT attenuation comes from hafnium itself and not the structure of hafnia, thus a strong crystal phase dependence on CT performance is not expected. The intensity-weighted mean hydrodynamic diameter and standard deviation values were evaluated using DLS. The hydrodynamic diameter for the as-synthesized hafnia nanoparticles was 13 ± 4 nm in toluene and 32 ± 12 nm in THF. The hydrodynamic diameters of the nanoparticles were tested in THF because this is the solvent used for the flash nanoprecipitation procedure. The reason for this difference between hydrodynamic diameters of nanoparticles suspended in toluene and THF is unclear.

Hafnia nanoparticle clusters (HNCs) were prepared through flash nanoprecipitation (FNP) using PLA-b-PEG as the block copolymer. Here, a custom-designed and 3D-printed multi-inlet-vortex-mixer (MIVM) was used. This significantly reduced the cost of the process and provided flexibility in mixer design. Dialysis against water was used to remove THF, and ultrafiltration was carried out to concentrate the HNCs. The physical appearance and hydrodynamic properties were assessed using TEM and DLS. Visualization from TEM images suggests the particles did form composite nanoparticle clusters, and that the clusters were well separated from each other

(Figure 1b). The arithmetic intensity-weighted mean diameter and standard deviation of 145 ± 46 nm obtained from DLS suggest successful preparation of HNCs that are dispersible in water. The zeta potential of the HNCs was determined at physiological pH of 7.2-7.4, revealing a zeta potential of ζ = 2.9 mV. This is consistent with other nanoparticles using PEG as the surface coating[31, 32]. Representative TEM images and hydrodynamic size distributions of the hafnia nanoparticles and HNCs are presented in Figure 1. The polydispersity index (PDI) for hydrodynamic diameters obtained from DLS was 0.12, 0.13, and 0.278 for particles in toluene, THF, and the HNCs, respectively.

To study the feasibility of adjusting HNC size over a wide range (size tuning), co-encapsulation of the hydrophobic homopolymer polylactic acid (PLA) was used. Triplicate samples were prepared for each PLA concentration, and the change in hydrodynamic size and size distribution were evaluated (see Figure S9). Here, a small-scale FNP process was used to evaluate a large number of FNP conditions while minimizing use of materials. The mass fraction (w_{PLA}) of PLA in the HNCs was calculated using equation 8, where *m* represents the mass of each component. The mass fraction, hydrodynamic diameter, PDI, and standard deviation were summarized in Table S1.

$$w_{PLA} = \frac{m_{PLA}}{m_{HfO_2}+m_{PLA-b-PEG}+m_{PLA}} \quad (2)$$

Samples were prepared in triplicate and hydrodynamic diameters are plotted against the mass fraction of PLA in Figure 2. The hydrodynamic diameter of the HNCs remains constant as the PLA mass fraction increases to 40% w/w and then increases with increasing PLA mass fraction above that value. The threshold mass fraction corresponds to PLA occupying ~40 % of the volume in the HNC. This behavior has been reported previously for composite nanoparticles consisting of gold crystals by Gindy et al.[25], who attributed it to the initial filling of spaces between the nanoparticles by the polymer for volume fractions below the threshold, followed by expansion of the inorganic core as volume fraction increases above the threshold value. For the FNP conditions used here, the initial hydrodynamic diameter is ~125 nm for 0 - 40% w/w PLA addition and reaches around 300 nm at 75% w/w PLA. However, as PLA mass fraction increases, the overall mass fraction of hafnia decreases, from 7.6% w/w hafnia for PLA mass fraction of 40% w/w to 3.6% w/w hafnia for PLA mass fraction of 75% w/w.

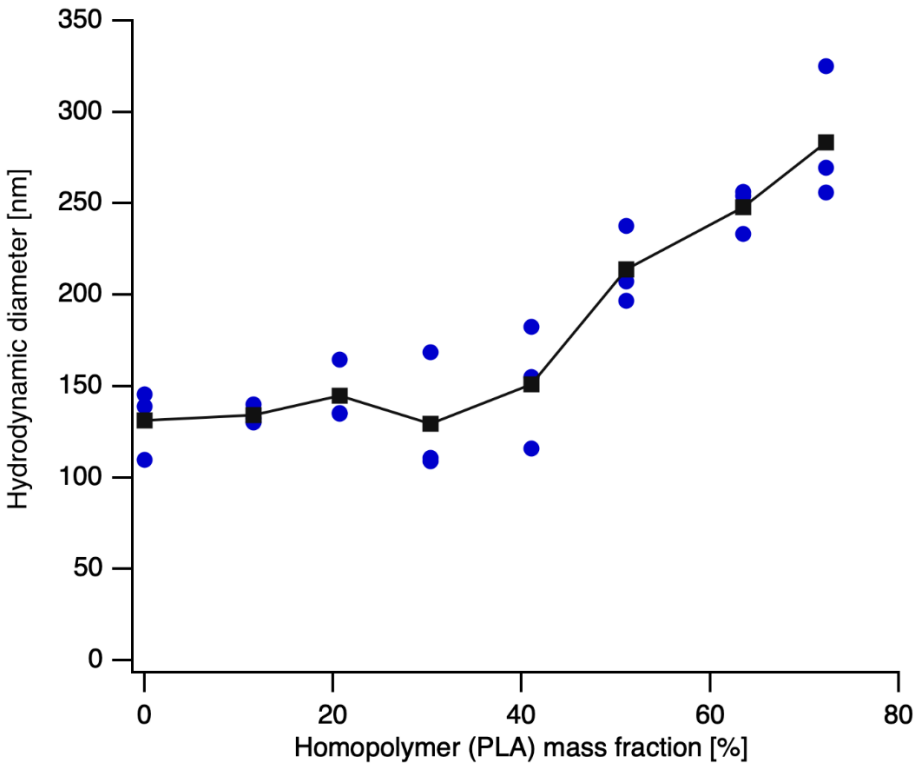

Figure 2. The arithmetic intensity-weighted mean diameter versus volume fractions of the co-core polymer PLA. The blue dots represent arithmetic intensity-weighted mean diameters for individual preparations in triplicate at each PLA volume fraction. The black squares are the average arithmetic intensity-weighted mean diameters at each PLA volume fraction.

3.2. Evaluation of CT contrast in different scanners

We evaluated the performance of the HNCs in two different scanner systems at various concentrations to verify their CT imaging capability. The scanners used were an IVIS® Spectrum In Vivo Imaging System with a CT module and an Aquilion ONE GENESIS scanner system. The CT module in the IVIS® Spectrum In Vivo Imaging System, which operates at 50 kVp, is commonly used in research to acquire reference anatomical information. The Aquilion ONE GENESIS scanner system is a human scale scanner used in hospitals.

Because the CT contrast in the HNCs primarily due to the X-ray attenuation of hafnium we formulated HNCs with the highest hafnium mass fraction (13%), corresponding to the condition where no PLA homopolymer was introduced. To have enough HNCs to prepare a dilution series from 50 mM to 0 mM at a volume of 400 µl for the phantom used in CT imaging acquisition, producing a larger amount of HNCs from the FNP process was required. As a result, a larger-scale pump FNP process was carried out as described in the methods section. Here, by increasing the raw materials input volume, a higher mass yield of the HNCs was achieved while maintaining the same properties as with the small-scale fabrication used in the sizing study. The hydrodynamic diameter (145 nm ± 46 nm) of the HNCs was evaluated and is shown in Figure 1d, suggesting negligible difference when compared to HNCs from the small-scale FNP process (Table S1). These results support the notion that FNP is a scalable method for the preparation of polymeric nanoparticles.

A commercially available and clinically used iodine-based contrast agent, Omnipaque, was used as a reference. For this purpose, we prepared a dilution series according to the molar concentration of iodine or hafnium from 1 mM to 50 mM. We used the iodine concentration provided by the manufacturer and hafnia content estimated from TGA data (shown in Figure S10.), as explained in the Methods section. To image the contrast agents in the Aquilion ONE GENESIS scanner, a plastic jar with a sample holder filled with water was used, avoiding a negative background. Additionally, a subtraction CT protocol was used to remove the background and water signal. As a result, the readings were already water signal subtracted. In contrast, the images acquired using the IVIS® Spectrum In Vivo Imaging System have air as the background. Therefore, manual water subtraction from the total signal was performed using the water signal acquired at the same equipment settings. Because the IVIS® Spectrum In Vivo Imaging System does not provide CT signal in a way that can be used to calculate X-ray attenuation in HU, no such calculation was conducted. In contrast, Aquilion ONE GENESIS scanner does provide such information. Hence, here we present the signal intensity for IVIS® Spectrum In Vivo Imaging System and HU for Aquilion ONE GENESIS scanner.

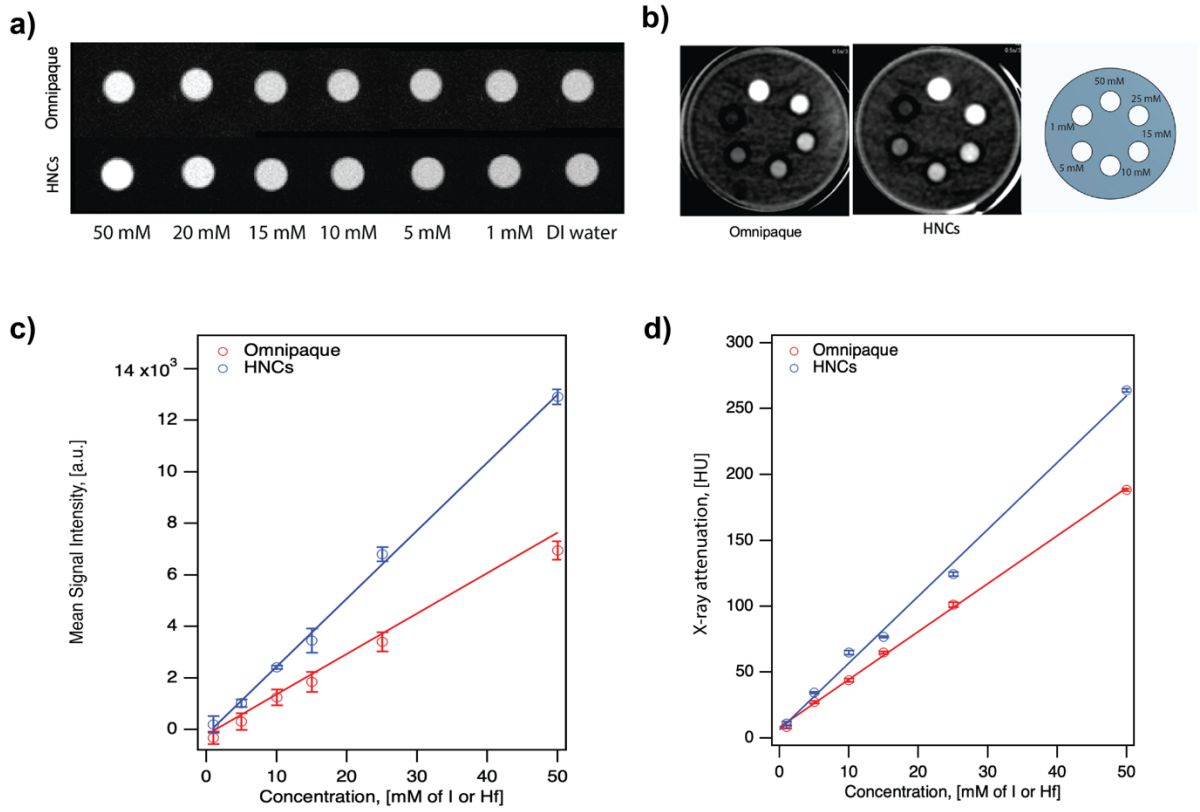

Figure 3. Evaluation of CT performance of HNCs and Omnipaque. a) grayscale images in IVIS® Spectrum In Vivo Imaging System CT module. b) grayscale images in clinical CT. c) X-ray attenuation measured in IVIS® Spectrum In Vivo Imaging System CT module. d) X-ray attenuation measured in clinical CT.

As seen in Figure 3a and b, the grayscale images from both scanners suggest that HNCs possess good CT contrast. We also observe that the HNCs have a stronger signal intensity (in the IVIS/CT) and X-ray attenuation (clinical CT) than Omnipaque at similar concentrations. The mean signal intensity versus concentration for both contrast agents in the IVIS/CT is shown in Figure 3c and the corresponding X-ray attenuation in the clinical scanner is shown in Figure 3d. Here, the linear relationship between X-ray attenuation and concentration in both systems for both contrast agents was clear. According to the fitting, the signal intensity of HNCs was 1.7x higher compared to Omnipaque in the IVIS® Spectrum In Vivo Imaging System and the X-ray attenuation was 1.4x higher in the Aquilion ONE GENESIS scanner. We note that the X-ray attenuation for HNCs in the current study (~275 HU at 50 mM at 120 kVp) is much smaller than that of hafnia nanoparticles reported in other studies (~900 HU at 50 mM at 45 kVp[6]). This can be due to the different CT scanners used for the studies. Because X-ray attenuation depends on the type of scanner, tube voltage of the scanner, field of view, and reconstruction algorithm, the X-ray attenuation from studies using different CT scanners and acquisition parameters cannot be compared directly[33].

3.3. Evaluation of colloidal stability of the HNCs

The colloidal stability of the HNCs in various media was investigated to demonstrate the stability of the composite nanoparticles. The visual appearance and hydrodynamic size of the particles were evaluated within a period of 24 hours at a concentration of 0.025 mg/ml. As seen in Figure S11, negligible changes in the hydrodynamic diameter and size distribution were observed for the HNCs in different media studied within 24 hours. The result suggests that the HNCs were stable in various media including PBS, DMEM, and DMEM+10% FBS at the concentration tested for at least 24 hours, consistent with steric stabilization due to the PEG component of the PLA-b-PEG block copolymer outer layer.

4. Conclusions

Computed tomography, a clinically used medical imaging modality, enjoys widespread use in the diagnosis and treatment of patients. An affordable contrast agent with tunable hydrodynamic diameter over a wide size range is desirable. In this study, hafnia nanoparticle clusters were formulated via flash nanoprecipitation using PLA-b-PEG as the block copolymer and PLA as the homopolymer and a 3D-printed multi-inlet-vortex-mixer. The physical and colloidal properties of the HNCs were evaluated. Size control over the range from 100 nm to 300 nm was demonstrated by adjusting the mass fraction of homopolymer in the flash nanoprecipitation streams. The intensity of the in-house formulated HNCs outperformed the clinical contrast agent Omnipaque by 1.7x and 1.4x in an IVIS® Spectrum In Vivo Imaging System and an Aquilion ONE GENESIS scanner using a SCT protocol, respectively. These results support flash nanoprecipitation as a simple and scalable process to produce inorganic nanoparticle CT contrast agents over a wide size range.

Reference:

1 *Radiation risk from medical imaging*, Sep 30, 2019).

2 Alexander, R. E. & Gunderman, R. B. EMI and the First CT Scanner. *Journal of the American College of Radiology* **7**, 778-781 (2010). https://doi.org:10.1016/j.jacr.2010.06.003

3 Jost, G., Pietsch, H., Lengsfeld, P., Hutter, J. & Sieber, M. A. The Impact of the Viscosity and Osmolality of Iodine Contrast Agents on Renal Elimination. *Investigative Radiology* **45**, 255-261 (2010). https://doi.org:10.1097/RLI.0b013e3181d4a036

4 Van Cauteren, T. *et al.* Improved enhancement in CT angiography with reduced contrast media iodine concentrations at constant iodine dose. *Scientific Reports* **8** (2018). https://doi.org:10.1038/s41598-018-35918-y

5 Nowak, T., Hupfer, M., Brauweiler, R., Eisa, F. & Kalender, W. A. Potential of high-Z contrast agents in clinical contrast-enhanced computed tomography. *Medical Physics* **38**, 6469-6482 (2011). https://doi.org:10.1118/1.3658738

6 McGinnity, T. L. *et al.* Hafnia (HfO2) nanoparticles as an X-ray contrast agent and mid-infrared biosensor. *Nanoscale* **8**, 13627-13637 (2016). https://doi.org:10.1039/c6nr03217f

7 Berger, M. *et al.* Hafnium-Based Contrast Agents for X-ray Computed Tomography. *Inorganic Chemistry* **56**, 5757-5761 (2017). https://doi.org:10.1021/acs.inorgchem.7b00359

8 Frenzel, T. *et al.* Characterization of a Novel Hafnium-Based X-ray Contrast Agent. *Investigative Radiology* **51**, 776-785 (2016). https://doi.org:10.1097/rli.0000000000000291

9 Hainfeld, J. F., Slatkin, D. N., Focella, T. M. & Smilowitz, H. M. Gold nanoparticles: a new X-ray contrast agent. *British Journal of Radiology* **79**, 248-253 (2006). https://doi.org:10.1259/bjr/13169882

10 Mahan, M. M. & Doiron, A. L. Gold Nanoparticles as X-Ray, CT, and Multimodal Imaging Contrast Agents: Formulation, Targeting, and Methodology. *Journal of Nanomaterials* **2018** (2018). https://doi.org:10.1155/2018/5837276

11 Ostadhossein, F. *et al.* Multi-"Color" Delineation of Bone Microdamages Using Ligand-Directed Sub-5 nm Hafnia Nanodots and Photon Counting CT Imaging. *Advanced Functional Materials* **30** (2020). https://doi.org:10.1002/adfm.201904936

12 Ostadhossein, F. *et al.* Dual purpose hafnium oxide nanoparticles offer imaging Streptococcus mutans dental biofilm and fight it In vivo via a drug free approach. *Biomaterials* **181**, 252-267 (2018). https://doi.org:10.1016/j.biomaterials.2018.07.053

13 Bao, J. F. *et al.* Multifunctional Hf/Mn-TCPP Metal-Organic Framework Nanoparticles for Triple-Modality Imaging-Guided PTT/RT Synergistic Cancer Therapy. *International Journal of Nanomedicine* **15**, 7687-7702 (2020). https://doi.org:10.2147/ijn.s267321

14 Nebuloni, L., Kuhn, G. A. & Muller, R. A Comparative Analysis of Water-Soluble and Blood-Pool Contrast Agents for in vivo Vascular Imaging with Micro-CT. *Academic Radiology* **20**, 1247-1255 (2013). https://doi.org:10.1016/j.acra.2013.06.003

15 Nanoprobes. <http://www.nanoprobes.com/products/AuroVist-Gold-X-ray-Contrast-Agent.html> (2017).

16 *Current rare earth element price.*, <https://strategicmetalsinvest.com/current-strategic-metals-prices/#:~:text=The%20current%20price%20of%20Hafnium%20is%20%241%2C741.10%20per%20kg.> (2022).

17 *Gold price*, <https://goldprice.org/> (2022).

18 Nallathamby, P. D., Sokolova, V., Prymak, O., Epple, M. & Roeder, R. K. in *Society for Biomaterials Annual Meeting 2018* (2018).

19 Li, Y. Y. *et al.* Gram-scale synthesis of highly biocompatible and intravenous injectable hafnium oxide nanocrystal with enhanced radiotherapy efficacy for cancer theranostic. *Biomaterials* **226** (2020). https://doi.org:10.1016/j.biomaterials.2019.119538

20 Hoshyar, N., Gray, S., Han, H. B. & Bao, G. The effect of nanoparticle size on in vivo pharmacokinetics and cellular interaction. *Nanomedicine* **11**, 673-692 (2016). https://doi.org:10.2217/nnm.16.5

21 Kemp, S. J., Ferguson, R. M., Khandhar, A. P. & Krishnan, K. M. Monodisperse magnetite nanoparticles with nearly ideal saturation magnetization. *Rsc Advances* **6**, 77452-77464 (2016). https://doi.org:10.1039/c6ra12072e

22 Park, J. *et al.* Ultra-large-scale syntheses of monodisperse nanocrystals. *Nature Materials* **3**, 891-895 (2004). https://doi.org:10.1038/nmat1251

23 Fuller, E. G. *et al.* Externally Triggered Heat and Drug Release from Magnetically Controlled Nanocarriers. *Acs Applied Polymer Materials* **1**, 211-220 (2019). https://doi.org:10.1021/acsapm.8b00100

24 Pinkerton, N. M. *et al.* Single-Step Assembly of Multimodal Imaging Nanocarriers: MRI and Long-Wavelength Fluorescence Imaging. *Advanced Healthcare Materials* **4**, 1376-1385 (2015). https://doi.org:10.1002/adhm.201400766

25 Gindy, M. E., Panagiotopoulos, A. Z. & Prud'homme, R. K. Composite block copolymer stabilized nanoparticles: Simultaneous encapsulation of organic actives and inorganic nanostructures. *Langmuir* **24**, 83-90 (2008). https://doi.org:10.1021/la702902b

26 Fuller, E. G. *et al.* Theranostic nanocarriers combining high drug loading and magnetic particle imaging. *International Journal of Pharmaceutics* **572** (2019). https://doi.org:10.1016/j.ijpharm.2019.118796
27 Liu, C. *et al.* Facile Single-Precursor Synthesis and Surface Modification of Hafnium Oxide Nanoparticles for Nanocomposite -Ray Scintillators. *Advanced Functional Materials* **25**, 4607-4616 (2015). https://doi.org:10.1002/adfm.201501439
28 Markwalter, C. E. & Prud'homme, R. K. Design of a Small-Scale Multi-Inlet Vortex Mixer for Scalable Nanoparticle Production and Application to the Encapsulation of Biologics by Inverse Flash NanoPrecipitation. *Journal of Pharmaceutical Sciences* **107**, 2465-2471 (2018). https://doi.org:10.1016/j.xphs.2018.05.003
29 Schindelin, J. *et al.* Fiji: an open-source platform for biological-image analysis. *Nature Methods* **9**, 676-682 (2012). https://doi.org:10.1038/nmeth.2019
30 Maldonado-Camargo, L., Unni, M. & Rinaldi, C. Magnetic Characterization of Iron Oxide Nanoparticles for Biomedical Applications. *Methods in molecular biology (Clifton, N.J.)* **1570**, 47-71 (2017). https://doi.org:10.1007/978-1-4939-6840-4_4
31 Liu, S. *et al.* Long circulating tracer tailored for magnetic particle imaging. *Nanotheranostics* **5**, 348-361 (2021). https://doi.org:10.7150/ntno.58548
32 Khandhar, A. P. *et al.* Evaluation of PEG-coated iron oxide nanoparticles as blood pool tracers for preclinical magnetic particle imaging. *Nanoscale* **9**, 1299-1306 (2017). https://doi.org:10.1039/c6nr08468k
33 Das, IJ *et al.* Computed tomography imaging parameters for inhomogeneity correction in radiation treatment planning. *Journal of Medical Physics*, **41**(1):3-11 (2016). http://doi.org:10.4103/0971-6203.177277

Supporting Information for

"Flash nanoprecipitation of hafnia nanoparticle computed tomography contrast agent"

Sitong Liu[1], Matthew Po[1], Anahita Heshmat[2], Evan Anguish[3], Jennifer Andrew[3], and Carlos M Rinaldi-Ramos[1,4,+]

Affiliations:

1. Department of Chemical Engineering, University of Florida, Gainesville, FL 32611, United States of America
2. Department of Radiology, University of Florida, Gainesville, FL 32610-0374, United States of America
3. Department of Material Science and Engineering, University of Florida, Gainesville, FL 32603, United States of America
4. J. Crayton Pruitt Family Department of Biomedical Engineering, University of Florida, Gainesville, FL 32611-6131, United States of America

[+]Corresponding author

Corresponding author email address: Carlos.Rinaldi@ufl.edu

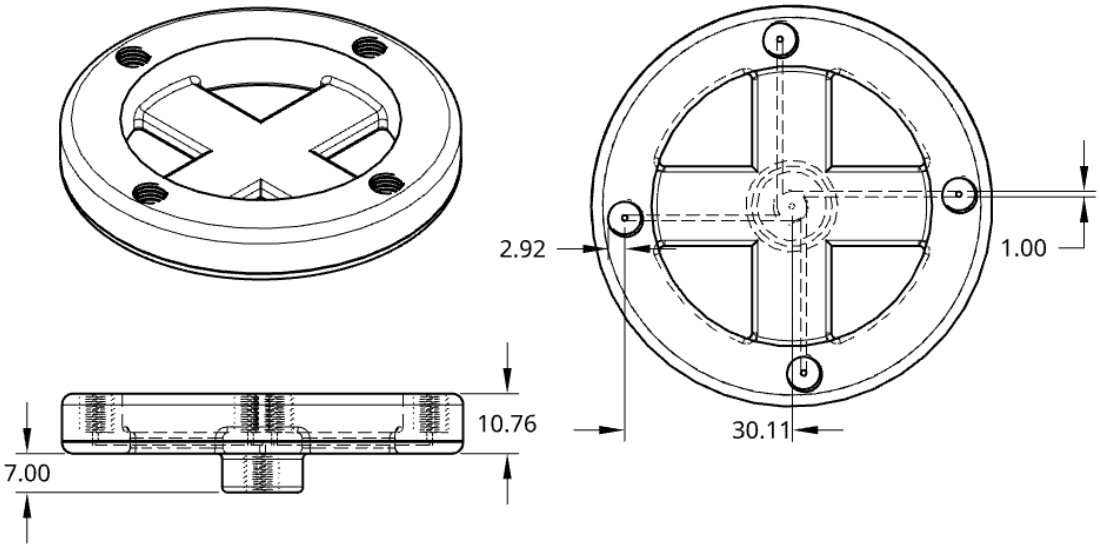

Figure S1. Custom-designed 3D-printed MIVM for the flash nanoprecipitation process used in the study. Specifications of this unit were adapted from Ref 23.

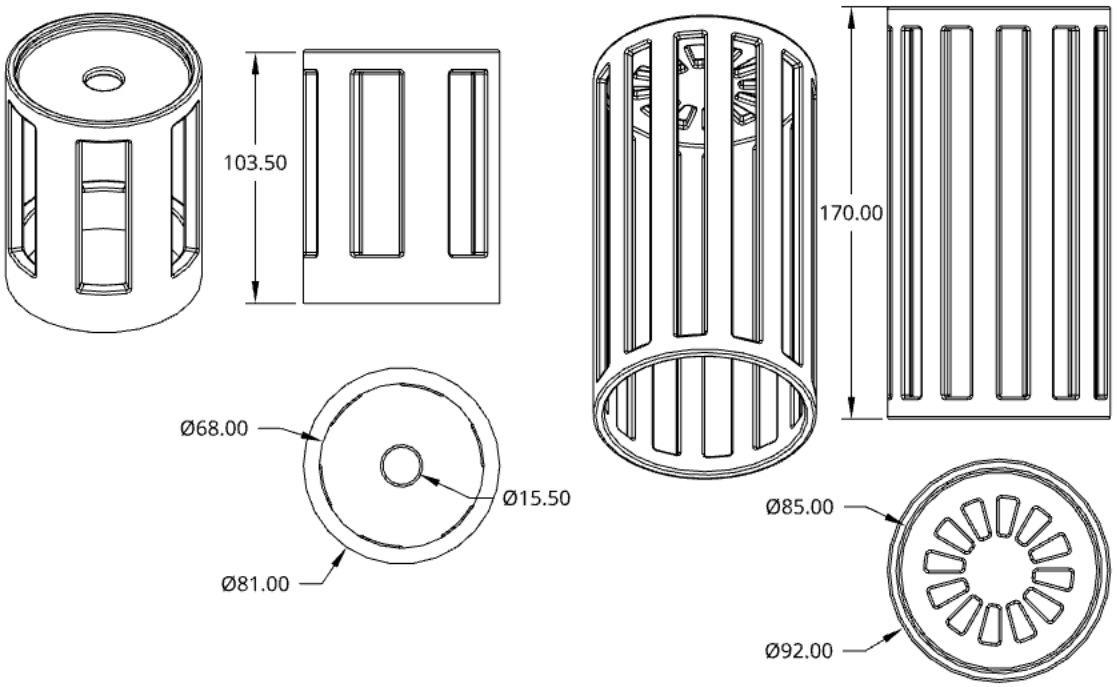

Figure S2. Custom designed 3D-printed holder and sleeve for MIVM used in the flash nanoprecipitation process used in the study.

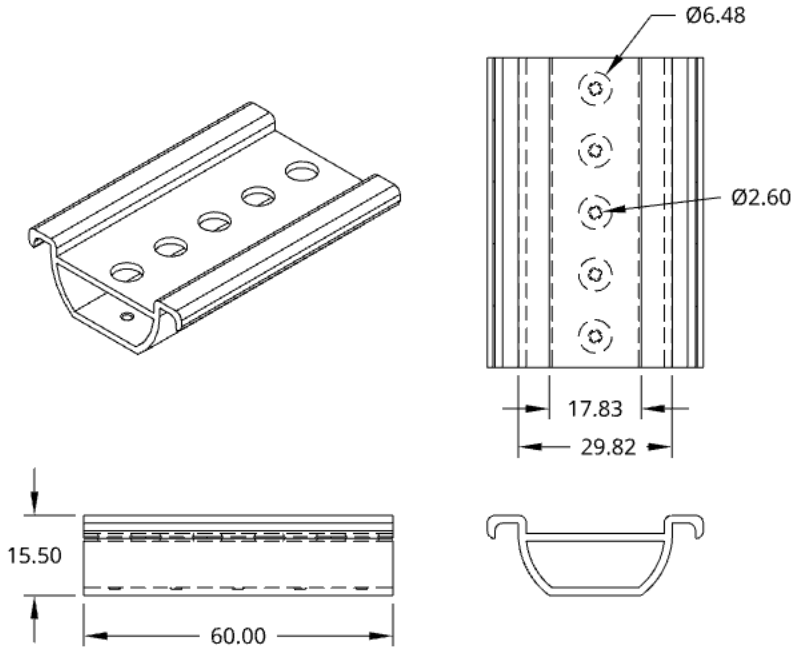

Figure S3. Custom designed 3D-printed holder for CT evaluation in PerkinElmer IVIS scanner.

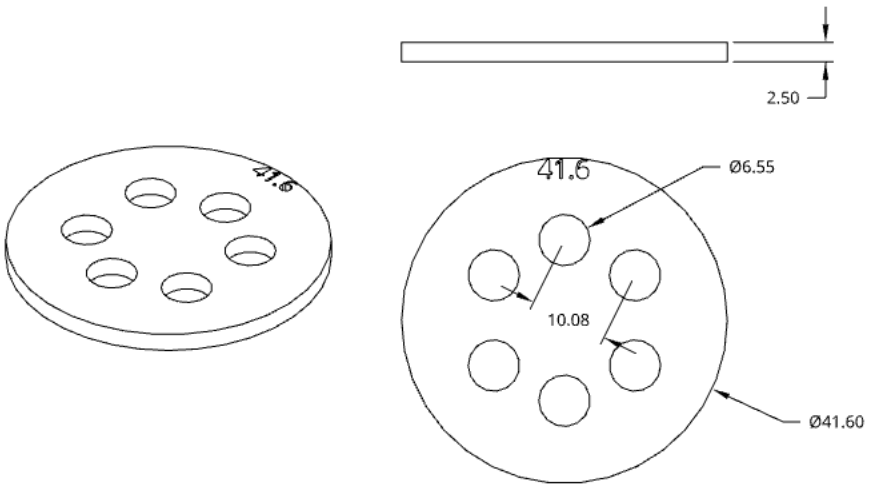

Figure S4. Custom designed 3D-printed holder for CT evaluation in Aquilion ONE GENESIS scanner to be coupled use with plastic jar.

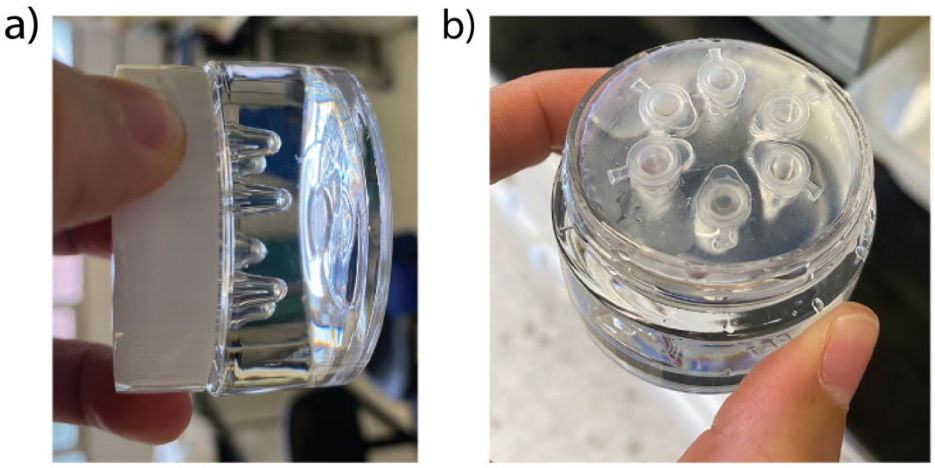

Figure S5. Configuration of sample holders in a plastic jar for CT evaluation. a) Orientation used in the measurements. b) Open jar with samples inside sample holder filled with water.

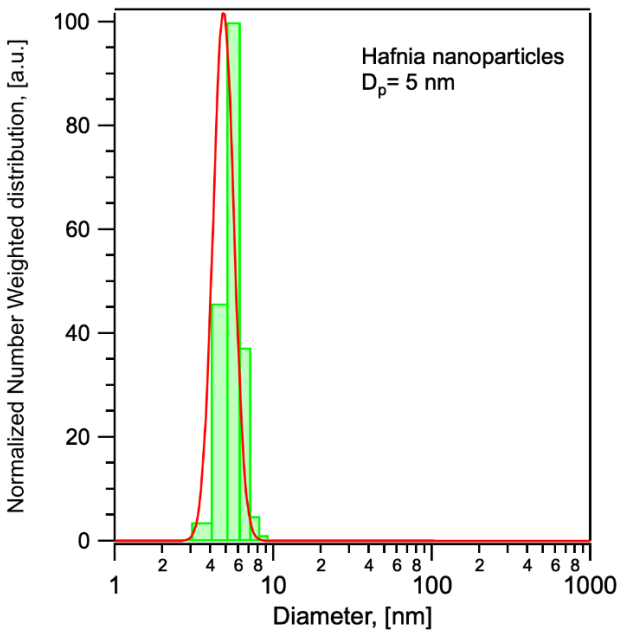

Figure S6. Physical size distribution of hafnia nanoparticles obtained from TEM. The arithmetic volume weighted mean diameter is 5.4 nm and the standard deviation is 0.82 nm.

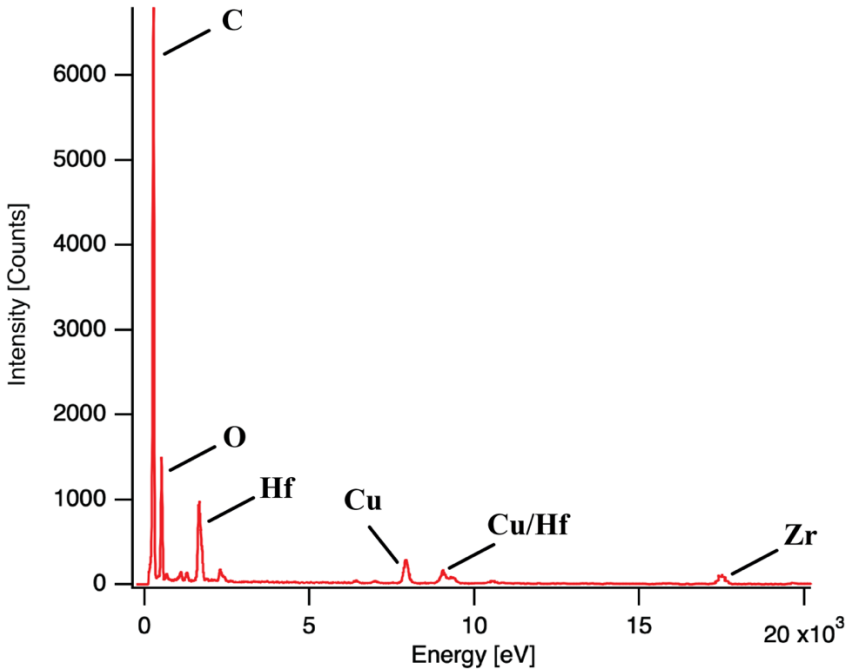

Figure S7. EDS obtained using a FEI TalosTM F200i S/TEM equipped with a Bruker XFlashTM 6T/30 windowless silicon drift detector EDS system at TEM mode. Cooper grid with carbon film was used for the filament.

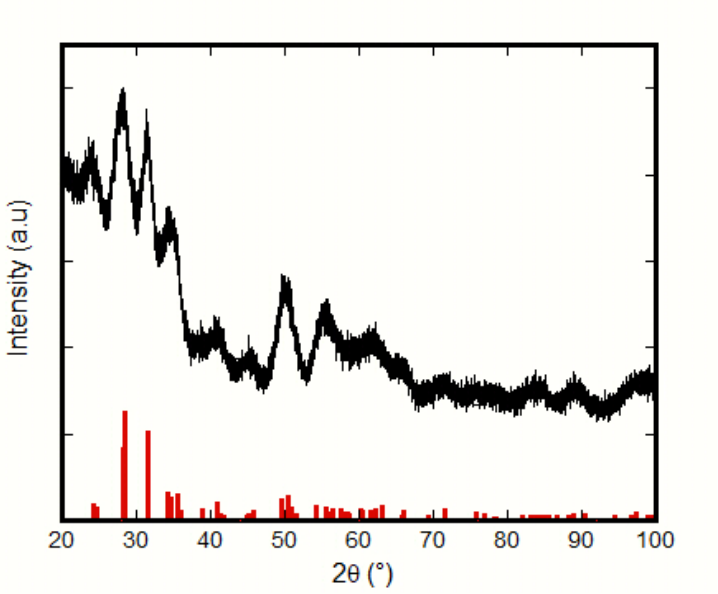

Figure S8. X-ray diffractogram of hafnia nanoparticles. The red vertical lines at the bottom correspond to reference (JCPDS 00-034-0104) for monoclinic phase hafnia.

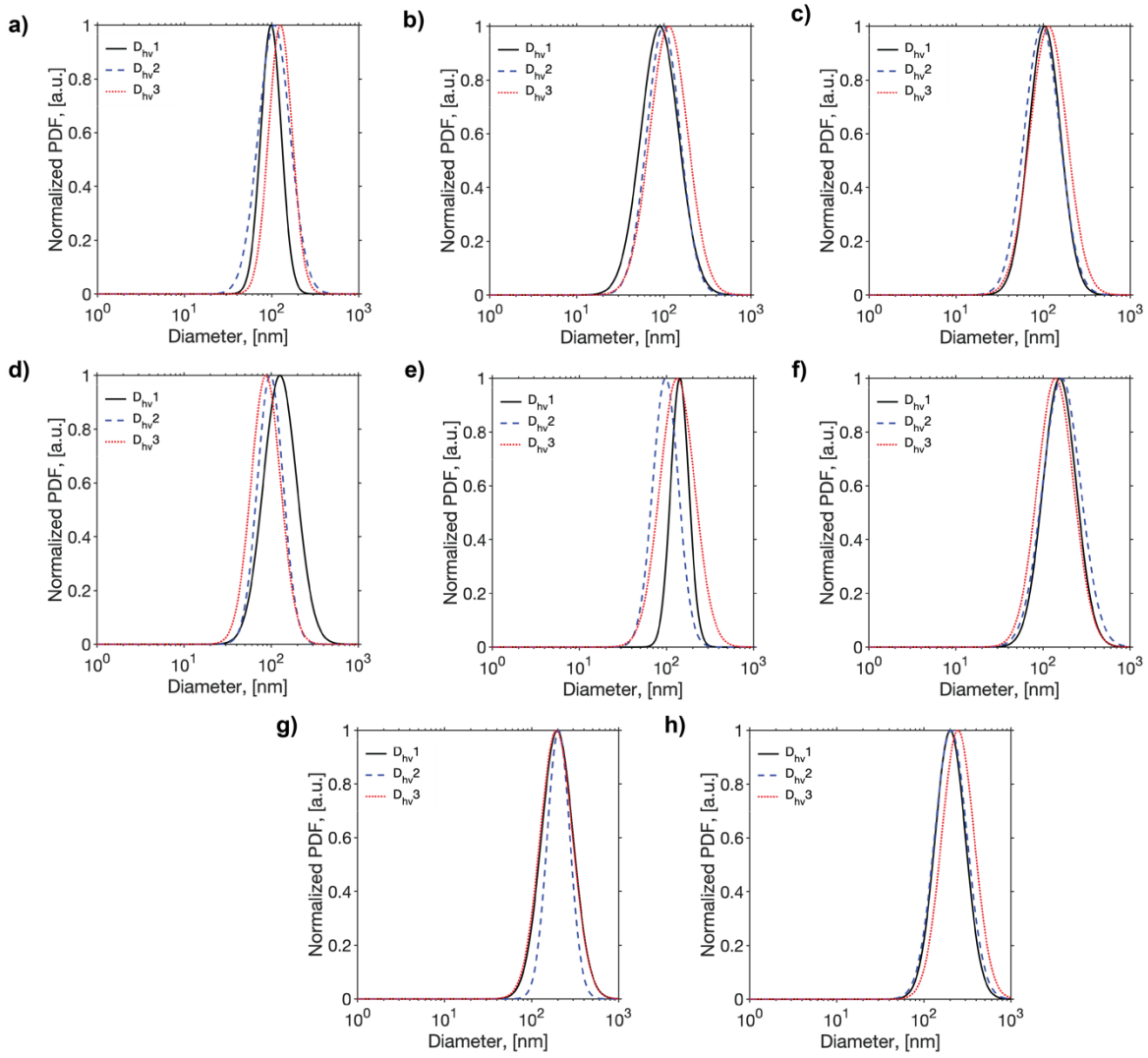

Figure S9. Hydrodynamic diameter distributions for HNCs at different co-core polymer mass fractions. In each figure, $D_{hv,1}$, $D_{hv,2}$, $D_{hv,3}$ represent triplicate under each co-core polymer mass fraction. a) 0%, b) 11%, c) 20%, d) 30%, e) 41%, f) 51%, g) 63%, h) 72%.

Table S1. Summary of hydrodynamic diameter size, standard deviation, and PDI for HNCs at different co-core polymer mass fractions.

PLA Concentration [mg/ml]	PLA Mass Fraction [%]	Hydrodynamic Diameter [nm]	Standard Deviation [nm]	PDI
0	0	109.6964412	69.00417	0.079
		139.0925031	92.14277	0.198
		145.4223238	92.54473	0.103
1.5	11.54	130.3460666	89.58545	0.286
		132.2629012	88.37522	0.218
		140.249784	96.39217	0.286
3	20.69	135.3243905	89.64656	0.195
		134.8624142	91.35062	0.249
		164.5212915	112.5154	0.269
5	30.30	168.6280384	112.6736	0.214
		110.9572626	73.50439	0.189
		109.0777804	71.38667	0.164
8	41.03	155.0106329	96.76581	0.059
		116.0897518	74.60172	0.123
		182.4468316	123.0092	0.232
12	51.06	207.5269476	138.665	0.21
		237.8478603	163.4703	0.289
		196.5803197	133.79	0.266
20	63.50	256.4719401	169.9016	0.192
		233.2642128	147.994	0.093
		254.0104445	168.9876	0.201
30	72.29	255.8399068	168.0988	0.175
		269.5638951	179.335	0.199
		325.2294537	216.3681	0.208

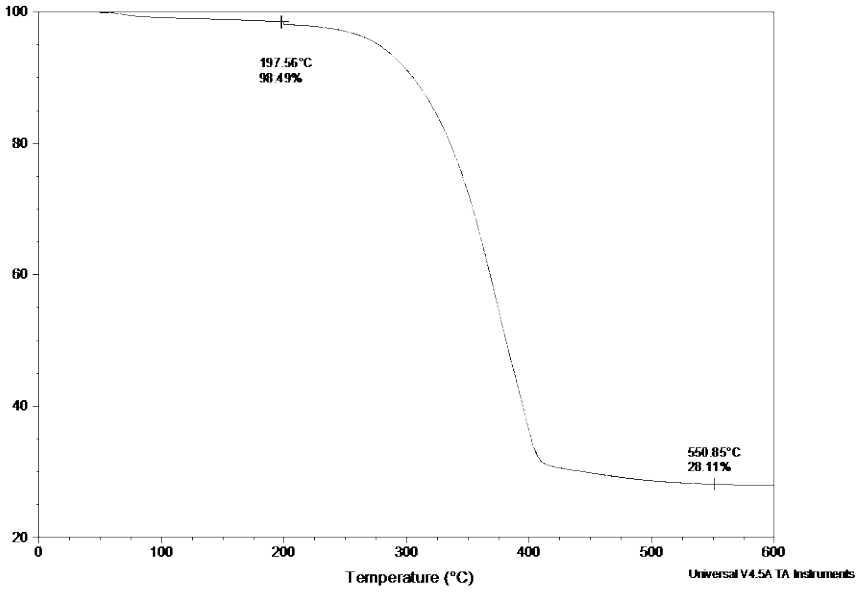

Figure S10. TGA scan of the HNCs to evaluate concentration for CT dilution series. The mass loss below 200 °C is considered moisture and solvent. Therefore, it was not considered in subsequent calculations. The organic mass percentage was 71.46%, determined by the weight loss percentage between 200 °C and 550 °C. The inorganic mass percentage was 28.54% for a total dry mass of 19.02 mg from 150 µl of the stock solution. The concentration of hafnia is calculated to be 36.2 mg/ml.

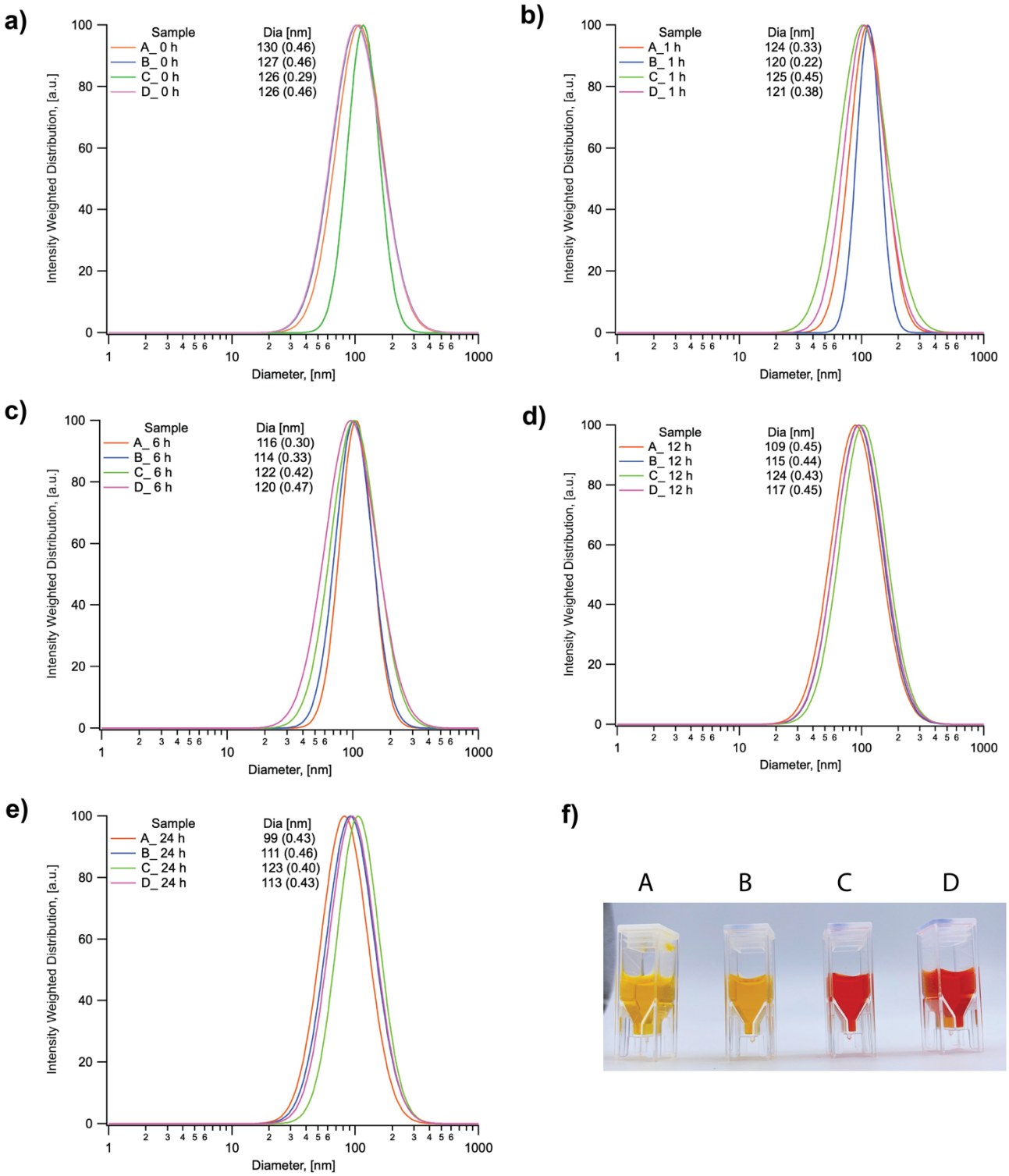

Figure S11. Hydrodynamic diameter and its distributions for HNCs in different media at different incubation time. The concentration of HNCs is 0.025mg/ml in all media. In each figure, A, B, C, and D represents DI water, PBS, DMEM, and DMEM+10% FBS. a) 0h, b) 1h, c) 6h, d) 12h, e) 24h, f) Pictures of DLS cuvettes containing HNCs in various media at 24 hours suggesting all solutions are still transparent clear with no sign of aggregation or settling of particulates.